RSC Advances

PAPER

View Article Online
View Journal | View Issue

Cite this: *RSC Adv.*, 2023, **13**, 22061

Electrochemical reduction of carbon dioxide to acetic acid on a Cu–Au modified boron-doped diamond electrode with a flow-cell system†

Millati H. Saprudin,[a] Prastika K. Jiwanti,[b] Deden Saprudin,[c] Afiten R. Sanjaya,[a] Yulia M. T. A. Putri,[a] Yasuaki Einaga[d] and Tribidasari A. Ivandini*[a]

Received 8th June 2023
Accepted 1st July 2023

DOI: 10.1039/d3ra03836j

rsc.li/rsc-advances

Boron-doped diamond (BDD) was modified with copper and gold particles by using an electrodeposition technique to improve its catalytic effect on CO_2 reduction in a flow system. The system was optimized based on the production of formic acid by the electroreduction process. At the optimum applied potential of −1.0 V (*vs.* Ag/AgCl) and flow rate of 50 mL min^{-1}, the copper–gold-modified BDD produced formic acid at the highest rate of 4.88 mol m^{-2} s^{-1} and a concentration of 15.93 ppm, while acetic acid was produced with a rate of 0.11 mol m^{-2} s^{-1} and a concentration of 0.47 ppm. An advantage of the flow system using the modified BDD was that it was found to accelerate the production rate of acetic acid as well as to decrease the reduction potential of CO_2. Furthermore, better stability of the metal particles was observed when using mixed copper–gold modification on the BDD surface than single modification by either metal. The results indicated that a flow system is suitable to be employed for electroreduction of CO_2 using the bimetal-modified BDD electrodes, especially with copper and gold as the modifying particles.

1 Introduction

Carbon dioxide (CO_2) exists naturally in the atmosphere and is one of the greenhouse gases produced by the combustion of fossil fuels. Increased human activity and energy demand have caused an increase in CO_2 gas in the atmosphere, which may cause global warming.[1] This high concentration of CO_2 gas in the atmosphere has attracted the attention of numerous researchers around the world, to suppress the emission of CO_2, to convert it into more valuable compounds that could be used as chemical stock, or to possibly convert it back to fuel. Various methods to convert CO_2 have been widely developed to produce valuable products effectively and efficiently, including chemical,[2] photocatalytic,[3,4] and electrochemical methods.[5–8] Among these methods, electrochemistry is one of the known methods involving a process that can be carried out at room temperature and pressure as well as neutral pH. In addition, the conditions of the reaction are easily adjustable.[9] The material used as the working electrode is one important factor, among many others, that is reported to influence the electrochemical reduction of CO_2. Accordingly, the use of many types of metals and non-metals for CO_2 electroreduction has been reported.[5–7,10,11]

Recently, boron-doped diamond (BDD) has been reported to be used as the working electrode in CO_2 electrochemical reduction. The unique properties of BDD, such as its high chemical and physical stability as well as its wide potential window, are believed to be key properties to suppress hydrogen evolution,[12,13] a reaction mechanism that usually interferes the reduction of CO_2.[14] The use of a BDD electrode for CO_2 electroreduction was reported to convert CO_2 into formic acid with high efficiency.[15,16] Furthermore, the modification of the BDD surface with various metals and bimetals has also been reported, leading to an increase in catalytic activity for CO_2 electroreduction.[7,14,17] Our previous reports have shown that modification of the BDD surface with copper particles can enable the conversion of CO_2 to C_2/C_3 compounds using a batch cell.[14,17] The interaction of copper to bind with carbon monoxide to form an intermediate that continuously reduces to hydrocarbon or alcohol was proposed as the mechanism.[18,19] Additionally, it was also reported that the electroreduction of CO_2 at a gold electrode generated carbon monoxide as the main product.[20,21]

In addition to the working electrodes, the electrochemical cell systems used for electrolysis have been reported to influence the CO_2 reduction product efficiency. A proper and well-

[a]*Department of Chemistry, Faculty of Mathematics and Natural Sciences, Universitas Indonesia, Kampus UI Depok, Jakarta, 16424, Indonesia. E-mail: ivandini.tri@sci.ui.ac.id*

[b]*Nanotechnology Engineering, Faculty of Advanced Technology and Multidiscipline, Universitas Airlangga, Surabaya 60115, Indonesia*

[c]*Department of Chemistry, Faculty of Mathematics and Natural Sciences, IPB University, Jl. Tanjung Kampus IPB Dramaga, Bogor 16680, Indonesia*

[d]*Department of Chemistry, Faculty of Science and Technology, Keio University, Yokohama 223-8522, Japan*

† Electronic supplementary information (ESI) available. See DOI: https://doi.org/10.1039/d3ra03836j

designed cell could produce the product in high yield and selectively. Two types of systems have been reported, namely, batch and flow systems. Employing a flow system, in which the electrolyte is pumped and flows through the electrode, thus improving the mass transfer of CO_2 to the surface of the working electrodes, was reported to influence the pH and CO_2 concentration on the electrode surface.[16,22] Accordingly, an increase in formic acid production from 71% to 94.7% by using a flow-system in a long-term use has been reported.[16]

The present research involves the electrochemical reduction of CO_2 at bimetallic copper and gold nanoparticles modified onto the surface of a BDD electrode in a flow-cell system. BDD modified with copper was selected because copper has the potential to generate organic compounds with more than one carbon,[16,17] while gold was selected to produce a high CO concentration to increase the copper electrode performance.[20,21] As expected, the presence of gold can increase the electrochemical conversion of CO_2 with a higher number of carbon atoms. Moreover, good stability of the electrode performance was observed, indicating that the developed electrode is promising for application to CO_2 reduction using a flow cell.

2 Experimental

2.1 Chemicals

$CuSO_4$ (98%), $HAuCl_4 \cdot 3H_2O$ (99.9%), KCl (99%), KOH (≥85.0%), H_2SO_4 (98%), HCl (37%), HNO_3 (70%), HCOOH (≥95%), CH_3COOH (99%), $HClO_4$ (70%), methanol (99.8%), ethanol (99.8%), and isopropanol (≥99.8%) were purchased from Sigma-Aldrich and applied without further purification. A simple lab water system (Direct-Q UV3, Millipore) with a maximum conductivity of 18 MΩ was used to produce the ultra-pure water.

2.2 Preparation of the working electrode

The BDD electrode was synthesized by using a chemical vapor deposition method as described in the previous report.[23] Methane gas was used as the carbon source and trimethoxyborane was used as the boron source; the ratio of boron to carbon in the precursor gas was maintained at 1%. The quality of the BDD was characterized using Raman spectroscopy (Fig. S1†); the spectrum showed a peak at 1333 cm^{-1} attributed to sp^3 carbon bonds and a pair of peaks at 500 and 1200 cm^{-1} related to disordered diamond without any sp^2 peak at 1500 cm^{-1}.[24] Prior to use, pre-treatment *via* ultrasonication in isopropanol and ultrapure water was applied to the BDD for 15 min each, followed by drying with N_2 gas. Copper-modified BDD (Cu-BDD) was prepared using a chronoamperometry technique in 0.1 M H_2SO_4 solution containing 1 mM $CuSO_4$ at a potential of −0.6 V (*vs.* Ag/AgCl),[17] whereas gold-modified BDD (Au-BDD) was prepared using the same technique in 0.1 M H_2SO_4 solution containing 1 mM $HAuCl_4$ at a potential of −0.2 V (*vs.* Ag/AgCl). Copper–gold-modified BDD (CuAu-BDD) was prepared at a potential of −0.6 V using 0.1 M H_2SO_4 solution containing 1 mM $CuSO_4$ and 1 mM $HAuCl_4$. The electrodeposition was carried out for various durations, *i.e.*, 60 s, 100 s or 300 s. All the prepared electrodes were then characterized using cyclic voltammetry (CV) and scanning electron microscopy-energy dispersive X-ray (SEM-EDS).

2.3 Electrochemical reduction of CO_2 and analysis of product

The reduction of CO_2 was performed using a flow cell with a coupled chamber divided by a Nafion 117 membrane (Fig. S2†). The working electrode (Cu-BDD, Au-BDD, or CuAu-BDD) was placed in one compartment. A solution of 0.5 M KCl containing CO_2 was placed in this compartment. The other compartment contained an Ag/AgCl system as the reference electrode and Pt wire as the counter electrode together with a solution of 0.5 M KCl as the electrolyte. Each compartment was connected by inlet and outlet lines to a reservoir with a volume of 1 L. To remove other gases in the solution, N_2 aeration was performed for 15 min. Next, a solution with dissolved CO_2 was prepared by conducting CO_2 aeration for about 5 min, which decreased the pH of the solution to around 3.9. A potentiostat (PGSTAT204; Metrohm Autolab) was employed for all electrochemical measurements. In the processes using the flow system, the electrolyte was pumped to flow through the electrode. The product was analysed using high-performance liquid chromatography (HPLC) (Welizer L600-DP6 with UV Vis Detector L600-UV) after 60 min of the electroreduction process. Inertsil ODS-3 (5 μm, GL Science) was used as the column and 0.1% $HClO_4$ was used for the mobile phase. The HPLC measurements of each standard solution of formic acid and acetic acid showed a chromatogram peak at a retention time of 2.1 min and 6.4 min, respectively. The standard chromatograms of acetic acid and formic acid are shown in Fig. S3.† An example of chromatograms containing formic acid and acetic peaks after the 60 min process is shown in Fig. S4† as the result of the electroreduction of CO_2 using a CuAu-BDD electrode at a potential of −1.0 V.

3 Results and discussion

3.1 Preparation of the solution for CO_2 aeration

A solution of 0.5 KCl containing CO_2 was used as the solution model to study the electroreduction of CO_2. Prior to the electroreduction process, N_2 aeration was carried out to remove other gas impurities from the solution. After N_2 aeration, no peak was observed in voltammogram of 0.1 M KCl at CuAu-BDD in the potential range from −2.0 V to 0.0 V (*vs.* Ag/AgCl) (Fig. 1, black line). A significant increase in the current at the onset potential of −1.7 V due to hydrogen evolution was confirmed. This result confirmed that the electrolyte was successfully cleaned and contained nitrogen only. Subsequently, the CO_2-aerated solution generated a well-defined reduction peak at a potential of around −1.5 V (*vs.* Ag/AgCl), indicating the reduction reaction of the dissolved CO_2 species in the electrolyte (Fig. 1). A slight shift in the onset potential of hydrogen evolution was observed due to the increase of the solution pH in the presence of CO_2, as the dissolved CO_2 formed carbonic acid.[14] Various CO_2 aeration times of 5, 15, and 30 min were

applied to obtain the optimum CO_2 dissolution. A higher current was observed for an aeration time of 15 min (Fig. 1, green line) indicating that a higher concentration of CO_2 could be dissolved in the electrolyte compared to those achieved using 5 and 30 min aerations (Fig. 1, red and blue lines, respectively). Accordingly, a solution of 0.5 M KCl aerated for 15 min with N_2 and then for 15 min with CO_2 was used as the standard solution to study the CO_2 electroreduction.

3.2 Preparation of the working electrodes

The working electrode was prepared *via* the modification of BDD films. The modification was performed *via* the electrochemical deposition of both copper and gold particles on the surface of BDD. Prior to the deposition, CV was performed in a 0.1 M H_2SO_4 solution consisting of 1 mM $CuSO_4$ as the source of copper and 1 mM $HAuCl_4$ as the source of gold to determine the parameters for the deposition. The voltammogram of the solution containing both metal cations is displayed in Fig. 2. Several reduction peaks were observed, including one at a potential of +0.6 V (*vs.* Ag/AgCl) as well as peaks at −0.1 V and −0.6 V. Accordingly, to provide for the simultaneous reduction of the copper and gold to be deposited on the surface of the BDD electrode, the higher reduction potential, *i.e.*, −0.6 V, was applied for the subsequent experiments. Similarly, this potential was applied to other BDD films using solutions of 0.1 M H_2SO_4 containing only 1 mM $CuSO_4$ or 1 mm $HAuCl_4$. A visible physical change with the formation of golden yellow spots was observed for the gold-modified BDD (Au-BDD) and the copper–gold-modified BDD (CuAu-BDD).

The electrochemical properties were measured to compare the BDD electrodes before and after the modification. Fig. 3 shows the differences in the voltammogram of BDD in 0.5 M KCl solution before and after electrodeposition. No peak was observed in the voltammogram of the unmodified BDD in the potential range from −2.0 V to 2.0 V (*vs.* Ag/AgCl), although a wide potential window from around −0.1 V to +0.2 V was observed (Fig. 3a), which is well known as an advantageous

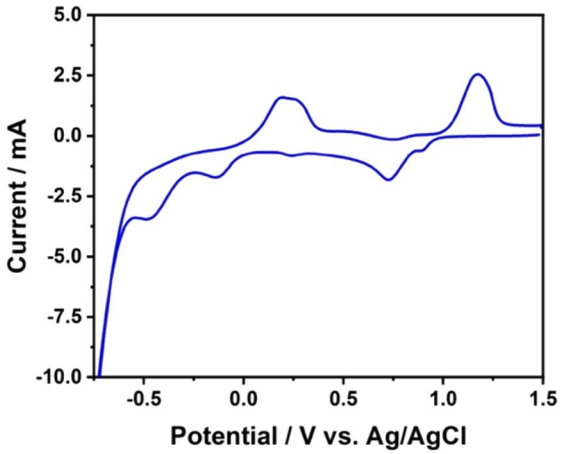

Fig. 2 Cyclic voltammogram of 0.1 M H_2SO_4 containing 1 mM $CuSO_4$ and 1 mM $HAuCl_4$ at the unmodified BDD electrode.

property of BDD.[9,20,21] After modification with copper, one pair of oxidation and reduction peaks was noted in the voltammogram at potentials of about +0.5 V and −0.5 V with a shift in the hydrogen evolution potential to more positive potential (Fig. 3b), whereas after modification with gold, the voltammogram shows an oxidation peak at +1.3 V and two reduction peaks at around +0.5 V and +1.0 V with a slight difference in the hydrogen evolution potential compared to the unmodified BDD (Fig. 3c). Additionally, the voltammogram of BDD after modification with copper and gold shows two oxidation peaks at around +0.2 V and +1.2 V and reduction peaks at around +0.6 V, −0.2 V and −0.6 V (Fig. 3d). The potentials of these peaks are very similar to the oxidation reduction potentials of copper and gold (Fig. 3b and c, respectively) indicating that both the copper and gold particles were deposited on the BDD surface. These results indicate that the Au and Cu particles deposited on the surface of BDD are in the bimetallic form since it shows individual peaks of Au and Cu. This result is in agreement with a report of synthesized Au–Cu nanoparticles on MWCNTs using

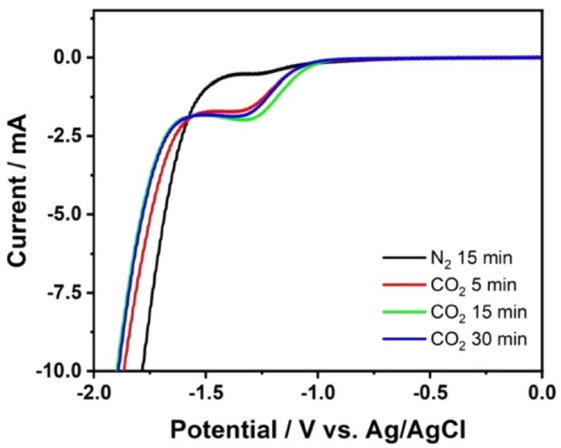

Fig. 1 Linear sweep voltammetry of 0.5 M KCl solution with various CO_2 aeration times using copper–gold-modified BDD. Scan rate was 100 mV s^{-1}.

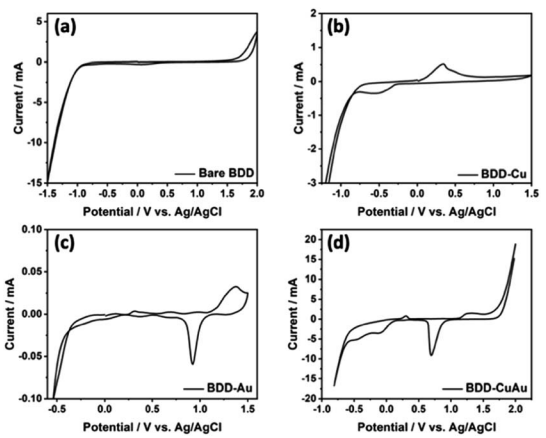

Fig. 3 Cyclic voltammograms of 0.5 M KCl solution at the unmodified BDD (a), as well as at the BDDs modified with copper (b), gold (c), and both copper and gold (d).

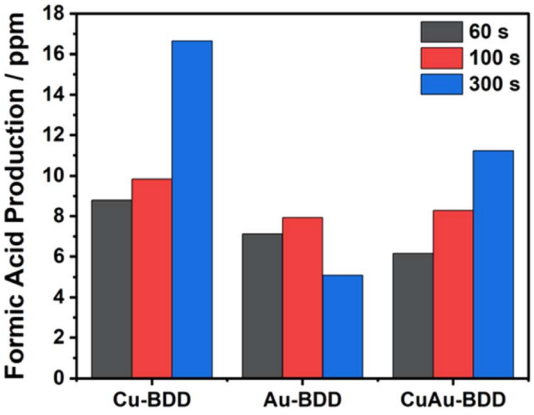

Fig. 4 Dependence of formic acid production on the deposition times of metals on the BDD surface.

Table 1 Elemental composition of the BDD films before and after the modifications

	Weight%			
Element	Unmodified BDD	Cu-BDD	Au-BDD	CuAu-BDD
C	88.80	98.88	93.51	98.20
O	13.20	0.94	3.59	0.30
Cu	N.A.	0.18	N.A.	0.12
Au	N.A.	N.A.	2.89	1.48

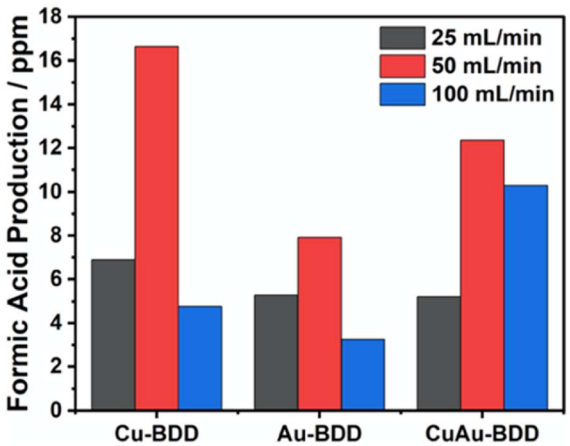

Fig. 5 Dependence of formic acid production on the flow rate in CO_2 reduction using the Cu-BDD, Au-BDD, and CuAu-BDD electrodes.

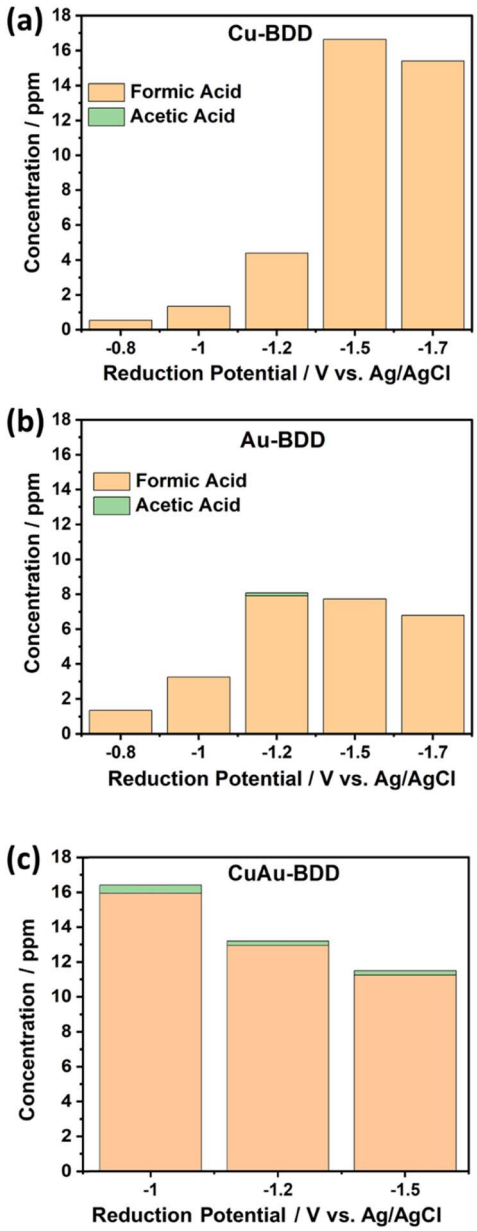

Fig. 6 Formic acid and acetic acid production on Cu-BDD (a), Au-BDD (b), and CuAu-BDD (c) at various reduction potentials in the flow electrochemical reduction of CO_2.

electrodeposition methods that are very similar to our methods.[25] In this report, the XPS spectra of the Au–Cu nanoparticles on the MWCNT exhibited Au 4f7/2 and 4f5/2 doublets with binding energies of 84.6 eV and 88.1 eV, respectively, and a Cu 2p peak with a binding energy of 935 eV, which are typically characteristic of Au^0 and Cu^0. This report confirmed that Au and Cu were deposited as bimetallic nanoparticles on the surface of MWCNTs. In addition, in this voltammogram, the hydrogen evolution potential was observed at a similar potential to that of Cu-BDD.

To study the optimum amount of copper and gold for deposition on the BDD surface, analysis of the products of the CO_2 electroreduction was performed. The electroreduction of CO_2 using Cu- and Au-BDD electrodes is expected to produce organic acids, alcohols, and gases. Formic acid is reported to be formed through an electron transfer process in which CO_2 receives an electron to become CO_2^- followed by protonation with an H^+ ion to form formic acid.[14] Additionally, the formation of acetic acid was proposed to involve two CO groups that are adsorbed on the electrode surface.[14] The adsorbed CO on

Table 2 Faradaic efficiency comparison of formic acid and acetic acid production at different applied potentials using Cu-BDD, Au-BDD, and CuAu-BDD

Electrode	Reduction potential (V *vs.* Ag/AgCl)	Conc. (ppm)		% faradaic efficiency	
		HCOOH	CH_3–COOH	HCOOH	CH_3–COOH
Cu-BDD	−0.8	0.54	0	30.08	0
	−1.0	1.35	0	30.32	0
	−1.2	4.40	0	12.97	0
	−1.5	16.64	0	33.92	0
	−1.7	15.40	0	9.09	0
Au-BDD	−0.8	1.35	0	21.71	0
	−1.0	3.25	0	35.57	0
	−1.2	7.91	0.17	39.59	2.58
	−1.5	7.73	0	10.73	0
	−1.7	6.79	0	7.63	0
CuAu-BDD	−1.0	15.93	0.47	40.31	3.63
	−1.2	12.93	0.26	17.70	1.10
	−1.5	11.23	0.25	13.26	0.92

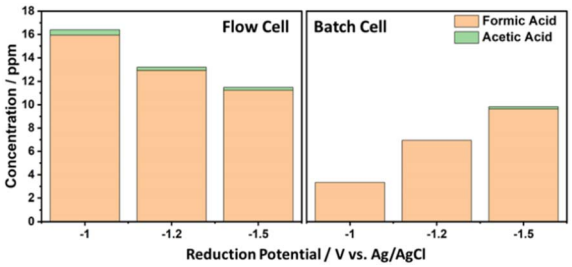

Fig. 7 Comparison of the flow cell and batch system on CO_2 reduction products using the CuAu-BDD electrode in 0.5 M KCl solution.

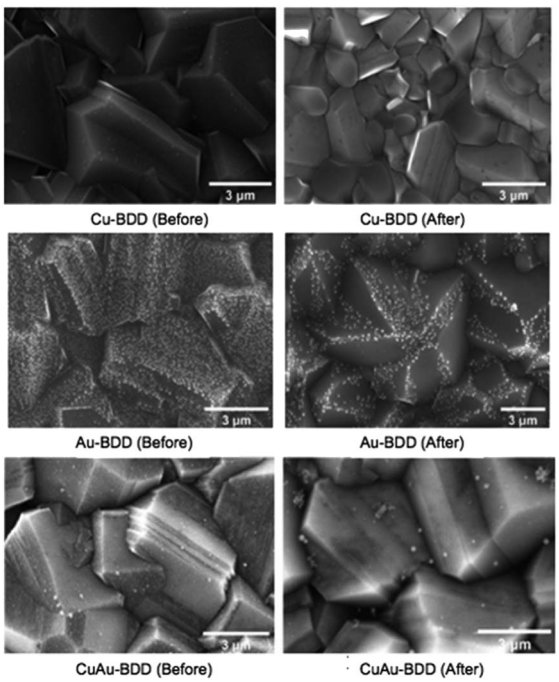

Fig. 8 SEM characterisation results of various working modified BDD electrodes before (left) and after (right) being used.

the electrode surface receives an electron transfer to form the acetic acid precursor. As the reported main product of CO_2 reduction was formic acid, optimization of the amount of copper and gold modification for the CO_2 electroreduction was conducted by observing the generated formic acid by using HPLC to measure the concentration of formic acid in the solution.[14]

The electroreduction of CO_2 was conducted at a potential of −1.5 V (*vs.* Ag/AgCl) using various deposition times for copper and gold as well as a mixture of copper and gold, namely, 60, 100 and 300 s. Increasing formic acid production was observed with increasing copper deposition time. The highest formic acid content was produced using copper deposition for 300 s, which generated 16.64 ppm formic acid (Fig. 4).

The SEM-EDS results show that the longer the applied deposition time, the greater the mass percentage of the deposited copper particles, resulting in an increase in the number of active species to catalyse the CO_2 electroreduction. Additionally, the modification of BDD with gold achieved the highest formic acid production at a deposition time of 100 s with 7.93 ppm formic acid (Fig. 4). At a deposition time of 300 s, the SEM-EDS results showed that the gold particles were agglomerated, resulting in a decrease in the gold electrocatalyst, thereby reducing the performance of the electrode in producing formic acid. In the case of modification with both copper and gold particles, an electrodeposition time of 300 s generated the highest formic acid production of 11.23 ppm formic acid. Accordingly, optimum deposition times of 300 s for copper electrodeposition, 100 s for gold electrodeposition, and 300 s for the electrodeposition of both copper and gold were selected for the subsequent experiments.

SEM-EDS characterization was performed to study the morphology of the BDD surface after the modification. The SEM images typically showed that small particles were deposited on the surface after the modification, while the analysis using EDS summarized in Table 1 indicated that copper and gold particles were successfully electrodeposited.

Table 3 Comparison of the different reported electrodes for CO_2 electroreduction

Electrode	System	Red time (min.)	Electrolyte	% faradaic efficiency	
				HCOOH	CH_3–COOH
BDD[31,32]	Batch	60	0.1 M NaCl	5.8	—
AuCu/GC[30]	Batch	20	0.1 M $KHCO_3$	2.5	—
Cu/GC[30]	Batch	20	0.1 M $KHCO_3$	11.5	0.5
Cu/Cu_2O[33]	Batch	60	0.5 M $NaHCO_3$	33.0	—
CuSn NPs/C-A[34]	Batch	15	0.1 M $KHCO_3$	71.5	—
SnO_2 nano-sheet/CC[35]	Batch	60	0.5 M $NaHCO_3$	87.2	—
Cd/Cu foil[36]	Flow	40	0.5 M $KHCO_3$	76.2	—
Oxide derived AuNP[37]	Flow	15	0.5 M $KHCO_3$	11	—
CuAu-BDD (this work)	Flow	60	0.5 M KCl	40.3	3.6

Table 1 shows that the surface of the unmodified BDD was composed of 96.8% (w/w) carbon and 3.20% (w/w) oxygen. Modification with metals typically decreases the oxygen content on the surface. Modification with copper decreased the oxygen content from 13.2% (w/w) to 0.94% (w/w), whereas the modification with gold decreased it to 3.59% (w/w). Modification with both copper and gold decreased the oxygen content to 0.30%. It has previously been reported that the surface of BDD films was terminated by hydrogen, as the films were prepared using a chemical deposition method under the hydrogen atmosphere.[13,26] The significant amount of oxygen on the surface of BDD was probably caused by the voltammetry treatment, which partially oxidizes the surface hydrogen terminations to give oxygen terminations.[13,26]

The decrease in oxygen content after modification indicated that the metal particles were deposited on oxygen atoms as the active sites. It seems the electrostatic interaction between the metal particles and the negative charge of oxygen drove the metal deposition on the oxygen sites of the surface.

Moreover, more gold than copper could be deposited on the BDD surface, which is reasonable as the reduction potential of copper, which is significantly more negative than the actual reduction potential of gold, was applied to deposit both gold and copper particles simultaneously.

Furthermore, the effect of the electrolyte flow rate was studied at a potential of −1.5 V (*vs.* Ag/AgCl) with Cu-BDD, Au-BDD and CuAu-BDD electrodes. Flow rates of 25, 50 and 100 mL min^{-1} were applied. Fig. 5 shows that for all the electrodes, increasing the flow rate to 50 mL min^{-1} increased the formic acid production, but production decreased at a flow rate of 100 mL min^{-1}. Theoretically, the increase in flow rate increases CO_2 mass transport, thereby increasing the production rate.[14] However, a technical problem occurs, as a flow rate higher than 50 mL min^{-1} increases a significant vibration in the electrolyte flow drive pump. This vibration affects the stability of the electrochemical work and triggers an increase in the hydrogen evolution reaction, resulting in a decrease in the CO_2 electroreduction performance.

The potential applied in this work so far was −1.5 V, considering that the onset potential for hydrogen evolution is around this potential. Applying a potential of −1.5 V seems to generate better performance for Cu-BDD than other electrodes. Accordingly, various applied potentials, including −0.8 V, −1.0 V, −1.2 V, 1.5 V and −1.7 V (*vs.* Ag/AgCl), were applied to optimize the reduction potential of CO_2 for all electrodes, as the applied potential is reported to strongly affect the selectivity products of the electroreduction of CO_2.[27] The products formic and acetic acid were used as the parameters of the electrode capability. Fig. 6 shows that Cu-BDD is a suitable working electrode to produce formic acid. The yield of formic acid initially increases as more negative potentials are applied. However, the formic acid production decreases at a potential of −1.7 V (*vs.* Ag/AgCl). A similar phenomenon also takes place when Au-BDD is used, with an increase in formic acid production, but the production of formic acid decreases at a potential of −1.5 V (*vs.* Ag/AgCl). At a more negative potential, the decrease in product efficiency is due to a great change in current density and high H_2 gas production, which causes the release of metal particles deposited on the BDD surface.

The CO_2 electroreduction performance using CuAu-BDD was observed under similar conditions. As the optimum reduction potentials of CO_2 electroreduction using Cu- and Au-BDD are −1.5 V and −1.2 V, respectively, potentials of −1.0 V, −1.2 V and −1.5 V (*vs.* Ag/AgCl) were applied when using CuAu-BDD as the working electrode. These results show that at all potentials, the CuAu-BDD electrode can produce formic acid and acetic acid (Fig. 6). The optimum reduction potential of −1.0 V (*vs.* Ag/AgCl) produces formic acid with a production rate of 4.88 mol m^{-2} s^{-1} with a concentration of 15.93 ppm, while the acetic acid production rate was 0.11 mol m^{-2} s^{-1} with a concentration of 0.47 ppm.

Table 2 shows a comparison of the CO_2 reduction products along with the acetic acid and formic acid production (concentration) and the faradaic efficiency (FE) of Cu-BDD, Au-BDD, and CuAu-BDD at different applied potentials. The highest FE for formic acid production (40.31%) could be obtained using CuAu-BDD at an applied potential of −1.0 V (*vs.* Ag/AgCl). Meanwhile, higher applied potentials of −1.5 V and −1.2 V for Cu-BDD and Au-BDD, respectively, were needed to achieve their optimum FE values of 33.92% (Cu-BDD) and 39.59% (Au-BDD). The highest formic acid production was achieved using Cu-BDD at a reduction potential of −1.5 V. However, the highest FE was

obtained using CuAu-BDD at a potential of −1.0 V. This phenomenon was probably due to the existence of gold on the prepared bimetal CuAu-BDD electrode. Gold particles provide better conductivity to further decrease the energy required for the electroreduction of CO_2, causing the optimum reduction potential to decrease around 33% from −1.5 V (the optimum potential applied for Cu-BDD) to −1 V. The results also indicated that the existence of the inert metal Au on the bimetal CuAu provides more stability in the electroreduction reaction of CO_2, resulting in a high FE of the CuAu-BDD electrode to produce formic acid. In addition, acetic acid was not observed at almost all the applied potentials when Cu-BDD or Au-BDD was used as the working electrode. The highest FE for acetic acid production (3.63%) was noted when using CuAu-BDD at an applied potential of −1.0 V.

The amount of acetic acid generated in this work is very low compared to the amount of formic acid generated. In fact, although some reports using Cu-based electrodes have shown the formation of acetic acid from the electroreduction of CO_2, it is not very easy to form acetic acid as 2 C and 8 H atoms are needed, as per the reaction below, while only 2 H atoms are needed to form formic acid. Accordingly, carbon monoxide or formic acid is generally formed by CO_2 reduction. Among the many solid electrodes, only copper and gold are reported to produce acetic acid. The reactions for producing both formic acid and acetic acid production are written as follows:[28,29]

$$CO_2 + 2H^+ + 2e^- \rightleftharpoons HCOOH \text{ (formic acid)}$$

$$2CO_2 + 8H^+ + 2e^- \rightleftharpoons CH_3COOH + 2H_2O \text{ (acetic acid)}$$

3.3 Comparison of flow systems and batch systems

The advantage of using the flow system was studied by comparing the CO_2 electroreduction of the flow system with that of the batch system using CuAu-BDD electrodes (Fig. 7). Using the batch system, formic acid can be produced at all potentials of −1.0 V, −1.2 V and −1.5 V (*vs.* Ag/AgCl). In addition, acetic acid can only be produced at −1.5 V (*vs.* Ag/AgCl) with a production rate of 0.04 mol m^{-2} s^{-1} and a concentration of 0.18 ppm. The use of the same electrodes and conditions in the flow cell system can produce acetic acid with a higher concentration, *i.e.*, 0.25 ppm, with a production rate of 0.06 mol m^{-2} s^{-1}. Accordingly, it can be concluded that employing a flow cell system for CO_2 electroreduction accelerates the production rate of acetic acid and at the same time reduces the reduction potential of CO_2 from around −1.5 V by using Cu-BDD to around −1.0 V by using AuCu-BDD.

3.4 Deposited metal stability for CO_2 electroreduction application

Further, the stability of the metal particles (copper and gold) at the modified BDD electrode for CO_2 electroreduction applications was examined. Characterisation using SEM-EDS was performed to indicate the stability of the copper and/or gold particles deposited on the BDD surface by comparing the particle composition before and after being used for CO_2 electroreduction. In general, the SEM-EDS results of the three modified BDD electrodes show a decrease in the copper and gold particle numbers after use for CO_2 electroreduction (Fig. 8). The EDS measurements indicated that a considerable decrease in mass occurred for Cu-BDD with a decrease of 44.44%. This significant decrease indicates that the copper particles are less stable on the surface of the BDD. A smaller but significant decrease was observed for the deposited gold in the Au- and CuAu-BDD electrodes, with lower gold particle release as the main reason. The results indicate that the gold particles have better stability on the BDD surface than the copper particles.

A comparison with reported electroreductions of CO_2 at various electrodes using batch and flow systems is summarized in Table 3. Cu-based electrodes have been widely used for the CO_2 reduction reaction due to their ability to not only produce HCOOH, but also to generate other products such as CO, CH_3COOH, and H_2. Additionally, their intrinsic properties as a stable conductive material provide the opportunity for the electrochemical setup to achieve high performance as a current collector, which contributes to the amount of product that can be produced in the electrochemical reaction. Additionally, to improve its activity and selectivity, combining Cu with other metal to form bimetallic catalysts has been widely investigated by other researchers. Comparison with other Cu- or Au- based electrodes that give HCOOH as a major product and CH_3COOH as a by-product shows that the developed CuAu-BDD electrode gave higher faradaic efficiency (FE) for formic acid and acetic acid production.

Furthermore, based on the comparison data in Table 3, the flow system with a proportional comparable electrode (AuCu/GC)[30] provides higher FE than the batch system. This phenomenon is attributed to the high performance from diffusion and charge transfer reaction on the surface of the working electrode, which was generated by the highest electrolyte mobility on the electrode surface, which decreases the diffusion layer and further increases the product yield of the reduction reaction. Therefore, developing the system from batch to flow has been proven to enhance the CO_2 electroreduction products.

In addition, this excellent performance takes place not only due to the influence of the bimetal materials and the setup of the system, but also due to substrate electrode used as the current collector. Compared to AuCu/GC and Cu/GC, the developed CuAu-BDD shows a higher FE for both HCOOH and CH_3COOH. The probable reason for this phenomenon is the wide potential window of BDD compared to GC, which would allow more hydrogen gas to be formed through the hydrogen evolution reaction. However, a higher formic acid FE was achieved when SnO_2 nanosheet/carbon cloth, CuSn NPs/C-A, and Cd/Cu foil were used as the working electrode. The higher surface area of electrode was probably the main reason. Accordingly, the optimization of the electro-active surface area is important to further enhance the formic acid and acetic acid production.

4 Conclusions

Copper and/or gold particles were successfully deposited on the surface of boron-doped diamond (BDD) to form copper-modified-BDD (Cu-BDD), gold-modified BDD (Au-BDD) and copper–gold-modified BDD (CuAu-BDD) to be employed as the working electrodes in the electroreduction of CO_2. Based on the formic acid production at the electrodes, the optimum deposition percentages were found to be 0.18% copper on Cu-BDD, 2.89% gold on Au-BDD, and 20% copper and 14.45% gold on CuAu-BDD. The flow system of CO_2 electroreduction showed an optimum electrolyte flow rate of 50 mL per minute with optimum applied potentials of −1.5 V, −1.2 V, and −1.0 V (*vs.* Ag/AgCl) for the Cu-BDD, Au-BDD, and CuAu-BDD electrodes, respectively. The highest production rates of formic and acetic acid were found using CuAu-BDD, with formic acid and acetic acid being produced with a rate of 4.88 mol m^{-2} s^{-1} and 0.11 mol m^{-2} s^{-1}, respectively. Faradaic efficiencies of 40.3% for formic acid and 3.6% for acetic acid could be obtained. The flow system of CO_2 electroreduction using AuCu-BDD was found to accelerate the production rate of acetic acid and to reduce the applied potential for CO_2 electroreduction from −1.5 V to −1.0 V potential (*vs.* Ag/AgCl). Better stability of the metal particles was also noted as well at Au-BDD and CuAu-BDD due to the better stability of the deposited gold.

Author contributions

M. H. S.: data curation, formal analysis, investigation, and writing; P. K. J.: conceptualization, supervision, validation, writing – review and editing; A. R. S.: investigation, writing – review, and editing; Y. M. T. A. P.: investigation, writing – review, and editing; Y. E.: conceptualization, supervision, validation; T. A. I.: conceptualization, supervision, validation, funding acquisition, writing – review and editing. All authors have given approval to the final version of the manuscript.

Conflicts of interest

There are no conflicts to declare.

Acknowledgements

This work is funded by Hibah PUTI Q2 Universitas Indonesia Grant No. NKB-653/UN2.RST/HKP.05.00/2022.

References

1 T. R. Anderson, E. Hawkins and P. D. Jones, *Endeavour*, 2016, **40**, 178–187.
2 P. Frontera, A. Macario, M. Ferraro and P. L. Antonucci, *Catalysts*, 2017, **7**, 59.
3 S. Chu, P. Ou, P. Ghamari, S. Vanka, B. Zhou, I. Shih, J. Song and Z. Mi, *J. Am. Chem. Soc.*, 2018, **140**, 7869–7877.
4 L. Qin, G. Ma, L. Wang and Z. Tang, *J. Energy Chem.*, 2021, **57**, 359–370.
5 C. Jia, K. Dastafkan, W. Ren, W. Yang and C. Zhao, *Sustainable Energy Fuels*, 2019, **3**, 2890–2906.
6 A. Bagger, W. Ju, A. S. Varela, P. Strasser and J. Rossmeisl, *ChemPhysChem*, 2017, **18**, 3266–3273.
7 P. K. Jiwanti and Y. Einaga, *Chem.–Asian J.*, 2020, **15**, 910–914.
8 D. Zang, Q. Li, G. Dai, M. Zeng, Y. Huang and Y. Wei, *Appl. Catal., B*, 2021, **281**, 119426.
9 R. Reske, H. Mistry, F. Behafarid, B. Roldan Cuenya and P. Strasser, *J. Am. Chem. Soc.*, 2014, **136**, 6978–6986.
10 D. Zang and H. Wang, *Polyoxometalates*, 2022, **1**, 9140006.
11 F. Ren, W. Hu, C. Wang, P. Wang, W. Li, C. Wu, Y. Yao, W. Luo and Z. Zou, *CCS Chem.*, 2022, **4**, 1610–1618.
12 T. A. Ivandini, W. P. Wicaksono, E. Saepudin, B. Rismetov and Y. Einaga, *Talanta*, 2015, **134**, 136–143.
13 T. Kondo, Y. Niwano, A. Tamura, T. A. Ivandini, Y. Einaga, D. A. Tryk, A. Fujishima and T. Kawai, *Electroanalysis*, 2008, **20**, 1556–1564.
14 P. K. Jiwanti, K. Natsui and Y. Einaga, *Electrochemistry*, 2019, **87**, 109–113.
15 K. Natsui, H. Iwakawa, N. Ikemiya, K. Nakata and Y. Einaga, *Angew. Chem.*, 2018, **130**, 2669–2673.
16 N. Ikemiya, K. Natsui, K. Nakata and Y. Einaga, *ACS Sustainable Chem. Eng.*, 2018, **6**, 8108–8112.
17 P. K. Jiwanti, K. Natsui, K. Nakata and Y. Einaga, *Electrochim. Acta*, 2018, **266**, 414–419.
18 Y. Hori and A. Murata, *Electrochim. Acta*, 1990, **35**, 1777–1780.
19 Y. Hori, H. Wakebe, T. Tsukamoto and O. Koga, *Electrochim. Acta*, 1994, **39**, 1833–1839.
20 S. Back, M. S. Yeom and Y. Jung, *ACS Catal.*, 2015, **5**, 5089–5096.
21 W. Zhu, R. Michalsky, Ö. Metin, H. Lv, S. Guo, C. J. Wright, X. Sun, A. A. Peterson and S. Sun, *J. Am. Chem. Soc.*, 2013, **135**, 16833–16836.
22 H. T. Ahangari, T. Portail and A. T. Marshall, *Electrochem. Commun.*, 2019, **101**, 78–81.
23 T. Yano, D. A. Tryk, K. Hashimoto and A. Fujishima, *J. Electrochem. Soc.*, 1998, **145**, 1870–1876.
24 T. A. Ivandini and Y. Einaga, *Chem. Commun.*, 2017, **53**, 1338–1347.
25 A. C. Bakir, N. Ahin, R. Polat and Z. Dursun, *J. Electroanal. Chem.*, 2011, **662**, 275–280.
26 K. Asai, T. A. Ivandini, M. M. Falah and Y. Einaga, *Electroanal*, 2018, **28**(1), 177–182.
27 D. Ren, J. Fong and B. S. Yeo, *Nat. Commun.*, 2018, **9**, 925.
28 R. Kortlever, J. Shen, K. J. P. Schouten, F. Calle-Vallejo and M. T. M. Koper, *J. Phys. Chem. Lett.*, 2015, **6**, 4073–4082.
29 C. W. Li and M. W. Kanan, *J. Am. Chem. Soc.*, 2012, **134**, 7231–7234.
30 D. Kim, J. Resasco, Y. Yu, A. M. Asiri and P. Yang, *Nat. Commun.*, 2014, **5**, 4948.
31 P. K. Jiwanti and Y. Einaga, *Phys. Chem. Chem. Phys.*, 2019, **21**, 15297–15301.
32 Y. Einaga, *Electrochemistry*, 2022, **90**, 101002.
33 C. W. Li and M. W. Kanan, *J. Am. Chem. Soc.*, 2012, **134**, 7231–7234.

34 P. Wang, M. Qiao, Q. Shao, Y. Pi, X. Zhu, Y. Li and X. Huang, *Nat. Commun.*, 2018, **9**, 4933.
35 F. Li, L. Chen, G. P. Knowles, D. R. MacFarlane and J. Zhang, *Angew. Chem., Int. Ed.*, 2017, **56**, 505–509.
36 Z. Chen, N. Wang, S. Yao and L. Liu, *J. CO_2 Util.*, 2017, **22**, 191–196.
37 Y. Chen, C. W. Li and M. W. Kanan, *J. Am. Chem. Soc.*, 2012, **134**, 19969–19972.